УДК 530.12, 681.7

СНИЖЕНИЕ ТЕПЛОВОГО ШУМА ЗЕРКАЛ В ДЕТЕКТОРЕ ГРАВИТАЦИОННЫХ ВОЛН. КРАТКИЙ ОБЗОР И НЕКОТОРЫЕ НОВЫЕ РЕЗУЛЬТАТЫ*

Пинто И. М.[a,b,c,1]

[a] Итальянский национальный институт ядерной физики (INFN).
[b] ЛВК Научное сотрудничество.
[c] Университет имени Федерико II, Неаполь 80138, Италия (Профессор пенсионер).

Оптические покрытия играют решающую роль в интерферометрических детекторах гравитационных волн. Представлен краткий, актуальный обзор соответствующих областей и результатов исследований, включая новые методы и результаты от исследовательской группы Автора.

Ключевые слова: Детекторы гравитационных волн, многослойные оптические покрыти, тепловой шум.

REDUCING THERMAL NOISE IN THE MIRRORS OF GRAVITATIONAL WAVE DETECTORS. A SHORT REVIEW AND SOME NEW RESULTS

Pinto I. M.[a,b,c,1]

[a] Istituto Nazionale di Fisica Nucleare (INFN), Italy.
[b] LVK Scientific Collaboration.
[c] University Federico II, Napoli 80138, Italy (retired professor).

Optical coatings play a crucial role in interferometric detectors of gravitational waves. A short up-to-date review of related research lines and results is proposed, including new methods and results from the Author's resarch group.

Keywords: Gravitational Wave Detectors, Optical Coatings, Thermal Noise.
PACS: 04.80.Nn, 42.79.Wc, 05.40.Ca
DOI: 10.17238/issn2226-8812.2023.3-4.229-246

1. Introduction

The spectral coverage of Earth-bound interferometric detectors of gravitational waves (GW), including LIGO [1], Virgo [2] and KAGRA [3] is set by seismic noise and laser shot noise, at low ($\lesssim$ 20Hz) and high ($\gtrsim$ 200Hz) frequencies, respectively. The noise level in the core ($20-200$Hz) observation-band is presently dominated by thermal noise in the highly reflecting (HR) coatings of the test masses terminating the optical cavities that make the interferometer arms. A typical 2nd-generation GW detector noise budget is shown in 1.

Coating thermal noise must be suitably reduced, to extend the detectors' range, and is needed to take advantage of already well developed quantum-noise reduction strategies [4].

Efforts to reduce coating thermal noise are ongoing, following different directions. This paper aims to provide a short, yet up-to-date summary of the relevant research lines and achievements, including key references to the topical Literature.

The needed modeling tools are summarized in Appendix-A and -B, where the relevant notation is introduced.

*Работа частично поддерживается «Национальным институтом ядерной физики» (INFN), Италия (проект Virgo). Work funded by "Istituto Nazionale di Fisica Nucleare"(INFN) of Italy (Virgo project).

[1] E-mail: pinto@sa.infn.it

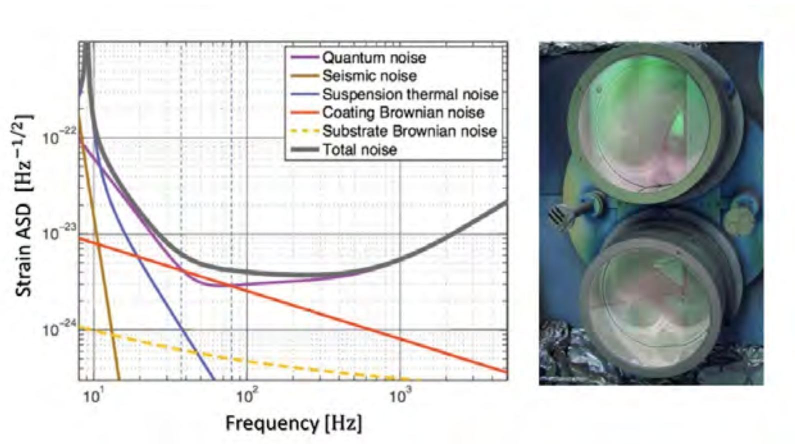

Рис. 1. Left: projected noise budget of 2nd generation GW detector (LIGO doc. P0900115). The strain amplitude spectral density and the observation bandwidth determine the detector sensitivity and its visibility range. Right: the aLIGO mirrors coated at CNRS-LMA (Lyon, FR); the coatings are deposited on 35cm⊘, 20cm thick fused silica substrates.

2. Materials and Methods

HR coatings consist of N_T homogeneous plane dielectric layers laid on a homogeneous half-space (substrate), as sketched in Figure A1, placed in high-vacuum.
Candidate coating materials, and coating design optimization methods are discussed below.
More *radical* routes to coating thermal noise (CTN) reduction include coating-free mirrors [5], compound mirrors [6] , and grating/diffractive reflectors [7]. These would require substantial modifications to existing detectors.

2.1. Coating Materials

The simplest reflective coating design consists of stacked identical pairs of high (H) and low (L) refractive index layers, each pair (doublet) having a total phase thickness of $\psi_H + \psi_L = \pi$ (Bragg condition) [8]. Using Appendix-A it is easily shown that the minimum number N_D of doublets for which the coating transmittance at a reference wavelength does not exceed a prescribed value is a non-increasing piecewise-constant function of the dielectric contrast n_H/n_L, which is minimum for $\psi_H = \psi_L = \pi/2$, i.e., for quarter-wavelength (QWL) layers.
On the other hand, as seen from eq. (B.1) of Appendix-B, coating thermal noise increases monotonically with the total metric thickness of the (L) and (H) layers, and the material noise-coefficients (B.2).
It is thus seen that “good” coating material pairs should feature a large optical contrast, and small noise-coefficients (B.2).

2.1.1 Material Downselection

Early material downselection surveys [9], [10] found that SiO_2 and Ta_2O_5 were the best available option for the L and H materials, featuring also low optical absorption (required to limit thermal deformation of the mirrors [11]) and diffusion. The introduction of Ti-doped (co-sputtered) Ta_2O_5 was an important step forward [12], yielding a substantial (roughly -30%) reduction of CTN power spectral density (PSD). Other material mixtures were tried, but failed to meet all needed requirements in terms of mechanical losses (thermal noise), optical absorption and scattering [13], with the notable exception of $SiO_2 : TiO_2$ [14]. A 2010 review of candidate coating materials, for use at ambient or cryogenic temperatures, can be found in [15].

2.1.2 Exploratory Material Searches

The range of optical coating materials for HR coatings is wide, and includes many oxides, halides, chalcogenides, nitrides, carbides, and a few amorphous metalloids. An exhaustive characterization of such materials and mixtures would require decades, and be fairly expensive.
Only a few beyond those already mentioned have been investigated so far, including, e.g., MgF_2 [16], AlF_3 [17], SiC [18] and GaN [19].
Also, a number of co-sputtered mixtures, besides $Ti:Ta_2O_5$, have been characterized, including, e.g., $SiO_2:HfO_2$ [20], $Sc_2O_3:Ta_2O_5$ [21], $TiO_2:Nb_2O_5$ [22], $ZrO_2:Ta_2O5$ [23], and $ZrO_2:TiO_2:Ta_2O_5$ [24]. See [25], [26] for comprehensive reviews of viable options. As of today, $Ti:Ta_2O_5$ and SiO_2 are still used in all working detectors.
In the last couple of years, much hope and effort has been put into the development of $TiO_2:GeO_2$ mixtures [27],[28]. Coating prototypes using $TiO_2:GeO_2/SiO_2$ doublets recently achieved remarkably low noise levels, a factor ≈ 0.5 lower in terms of PSD compared to the current $Ti:Ta_2O_5/SiO_2$ based aLIGO design [29]. This is not far from the 0.25 design goal of aLIGO+, but optical absorption is still too high (by a factor ≈ 2), and defects (bubbles, cracks, delamination) and aging phenomena have been observed [30], whose origin and remediation are not yet fully understood.
Titania-Silica ($TiO_2:SiO_2$) mixtures could be another option, perhaps less-critical, and are also under active development [31].

2.1.3 Nanolayered Mixtures

Nanolayered metamaterials are an alternative to co-sputtered mixtures. Modeling their relevant optical and viscoelastic properties is straightforward [32], and their technology faces almost no challenge. Nanolayering $SiO_2:TiO_2$ was shown in [33] to hinder crystallization of TiO_2 during post-deposition annealing, thus preventing the ensuing blow-up of optical (and mechanical) losses [1].
It was further found that in nanolayered $SiO_2:TiO_2$ films the mechanical loss-peak observed in Silica films at cryogenic temperatures is almost suppressed [35], [36]. Nanolayered mixtures with high and low refractive index have been discussed [37], [38].
Nanolayered films have been deposited by several Groups. The key role of glass-forming (Silica) nanolayers in preventing interdiffusion has been noted [39]. It has been confirmed that, for some materials, nanolayered mixtures may exhibit lower mechanical losses than their (isorefractive) cosputtered counterparts [40].
In a solid-state perspective, nano-layering can be seen as a wavefunction-confinement strategy, providing a simple *band-gap engineering* tool, whereby both the refractive index and the extinction coefficient of the composite can be tuned almost indendently over relatively wide ranges [41].

2.1.4 Mixture Modeling and Process Engineering Tools

Effective medium theories (EMT) [42] provide a simple yet accurate modeling tool to predict the optical properties of mixtures [43]. A formal extension of EMT to visco-elastic properties was formulated in [44], and used in [45] to model $Ti:Ta_2O_5$.
At a more fundamental level, our working knowledge of optical and viscoelastic properties and their interplay [46], [47] is improving, thanks to progress in molecular modeling [48], [49] that sheds light into the link between microscopi structure/morphology and macroscopic properties, [50]-[52], and in perspective, may suggest criteria for *engineering* the materials [53].
Molecular/atomistic modeling has been recently used to simulate film deposition processes [54]-[56]. This may help understanding the non obvious observed dependence of coating properties on deposition

[1] Early coating prototypes based on TiO_2/SiO_2 Bragg doublets were spoiled by almost complete crystallization after annealing [34].

technology, assisting gases, substrate heating, etc., and allow for considerable time saving in process optimization.

2.1.5 Material Metrology

Research on optical coating materials for interferometric GW detectors triggered important advances in the related Metrology.
The development of techniques [57], [58] for measuring extremely low optical absorption (photon common path interferometry, PCPI) and scattering [59], the invention of new strategies for measuring the thermoelastic and thermorefractive coefficients in thin films and multilayers [60], [61], the introduction of improved setups for multi-mode mechanical ringdown measurement in thin films [62] and the extraction of bulk and shear elastic moduli thereof [63], and of reliable instruments for the *direct* measurement of the thermal noise power spectral density in HR optical coatings and optical thin films [64]-[68] are noteworthy examples.

2.1.6 Crystalline Coatings

High-stakes research work has been focused on crystalline materials, offering a potential large reduction of thermal (Brownian) noise [69] in HR coatings. Two possible material options have been explored so far : $GaP/AlGaP$ doublet-stacks grown on (lattice-matched) c-Silicon substrate - see [70]-[72], and $GaAs/AlGaAs$ doublet-stacks grown on $GaAs$ and substrate-transferred [73] - see [74] for a recent status report, and a review of relevant technological challenges.
It has been long assumed that thermal noise in crystalline coatings would be dominated by thermo-optic (TO) and photo-thermal (PT) fluctuations. The thermoelastic and thermorefractive components of TO and PT noise [75] may cancel out in part, insofar as they add coherently [76], and cancellation can be maximized by suitably optimizing the layer thicknesses [77]. However, recent measurements in $GaAs/AlGaAs$ coatings found additional birefringence-related extra noise [78], and highly spatially-correlated excess-noise [79], that need to be addressed [2].

2.1.7 Silicon Nitrides

Silicon Nitride films have been proposed as candidate materials for both the H and L layers in binary coatings [80]. Plasma-enhanced chemical vapor deposition (PECVD - a technology that has almost no substrate-size limitations) can be used to produce non-stoichiometric SiN_x films with flexible composition, yielding a wide range of refractive indexes, with fairly low mechanical loss angles ($\phi \lesssim 10^{-4}$).
A recently introduced NH_3-free PECVD process has further improved the material parameters. Films with $n \approx 2.68$ and $\kappa \approx 1.2 \cdot 10^{-5}$ @1550nm, with $\phi \lesssim 10^{-4}$ down to cryogenic temperatures have been produced [81].
Silicon Nitrides deposited via IBS [25] and IBD [82] are being developed too, and look promising.

2.1.8 Amorphous Silicon

Amorphous silicon has been indicated as an excellent candidate for multimaterial coatings [83]-[87], featuring a large refractive index ($n = 3.5$@1550nm), and low mechanical losses, both at ambient ($\phi \approx 10^{-4}$ at 290K) and cryogenic temperatures ($\phi \approx 2 \cdot 10^{-5}$ @ 20K).
Current efforts are focused on reducing its optical absorption [88], and increasing its maximum annealing temperature [89]. As noted in Section 3, aSi could be an effective ingredient for ternary coatings even assuming its optical extinction to remain relatively large (e.g., $\kappa \approx 10^{-3}$); however, increasing its maximum annealing temperature is mandatory, in order to bring the mechanical losses of the other

[2] Spatial fluctuations correlation across the coating face would make the use *wide* beams ineffective to reduce noise.

materials in the coating to comparably (low) values.
As a conclusion, several options exist, with different degrees of reliability and knowledge, for future coating materials, both at ambient and cryogenc temperatures. As of today, Silica and Ti-doped Tantala remain the best known and reliable candidates low- and high-index materials. However, new materials may provide better performances, once stable and reliable deposition protocols are found, especially if used in the advanced optimized designs discussed in the next sub-Section.

2.2. Coating Design Optimization

An early insightful analysis of HR binary coatings consisting of identical cascaded doublets of lossy dielectrics, aimed at determining the doublet structure and the number of doublets yielding the largest reflectance at a given wavelength was introduced by Zel'dovich and Vinogradov [90].
The more general case of m-ary coatings consisting of stacked m-tuplets of $m > 2$ lossy dielectrics was later studied by Larruquert in a series of papers [91]-[93]. He notably pointed out that in order to achieve the largest reflectance, the materials in each m-tuplet should be orderd so as to turn *clockwise* in the complex refractive-index plane when moving toward the substrate from one layer to the next in each m-tuplet.
In the present context the optimization goal is minimizing coating thermal noise at some assigned transmittance, while also keeping coating absorbance below some prescribed level, and the previous results are not directly applicable.
Robust (genetic) optimization shew that even in this case, the optimal (binary) coating design consists of almost identical stacked quasi-Bragg doublets, where the thickness of the noisier material ($Ti\!:\!Ta_2O_5$, at the time of the study) is trimmed to the advantage of the other one (SiO_2). Only a few layers near the coating top and bottom may deviate (slightly) from the above regularity in the optimized design, and can be adjusted sequentially [94]. This suggested a simple iterative coating design procedure [8] that was experimentally validated [95], and eventually adopted to build the aLIGO mirrors [96] used in the first GW observations [97]. A more refined analysis, including subtler effects in [98], led to equivalent results.
Some general bounds to the noise reduction (compared to the simplest QWL design) achievable by the above optimization were obtined in [99].

3. Ternary Coatings: Rationale and Early Results

Using three different materials in HR oatings for GW detectors was first suggested in [100], [101], in connection with the development of aSi, and demonstrated in [103].
Denote as L, H and H' three different materials, and assume that

$$n_{H'}/n_L > n_H/n_L,\ b_L < b_{H'} < b_H,\ \kappa_{H'} \gg \kappa_H \sim \kappa_L. \tag{3.1}$$

where $n - \imath\kappa$ is the complex refractive index, and b the noise coefficient (B.2). In view of (3.1) a coating using $[L|H']$ doublets would exhibit lower mechanical losses (hence noise) but larger absorbance compared to a coating using $[L|H]$ doublets feauring the same transmittance.
The basic idea proposed in [100], [101] is using H' only in the doublets close to the substrate, where the field intensity is sufficiently low to make the larger extinction coefficient of H' harmless [3]. The resulting coating will thus consists of a stack of N_t doublets $[L|H]$ laid on top of a stack of N_b doublets $[L|H']$.
In the simplest case, all layers can be QWL (i.e., with phase thickness $\pi/2$), and the design optimization problem has only two degrees of freedom, (N_t, N_b).
By analogy with the binary case, a better coating design may be obtained by assuming the phase thicknesses

$$\psi_{L,H} = \pi/2(1 \pm \xi),\ \psi_{L,H'} = \pi/2(1 \pm \xi'), \text{with } \xi, \xi' \in (0, 1(\tag{3.2}$$

[3]It was also suggested to put a crystalline layer (or a few high-contrast, low-noise doublets) on top of the coating stack, to further reduce the field transmitted beyond the first layers [102].

whereby all doublets fulfill the Bragg condition. In this case the design/optimization problem has four degrees of freedom (N_t, N_b, ξ, ξ').
The performance of doublet-based ternary designs has been discussed in [104], where also the more general cases of *quasi*-Bragg doublets, and end-layer tweaked stacks have been considered, and shown to provide only marginally better results. The main results of the analysis in [104] are illustrated in Figure 2, that refers to optimized ternary coatings with QWL layers, using SiO_2 (L), $Ti\!:\!Ta_2O_5$ (H), aSi (H') on cSi substrate operating at 1550 nm. The figure shows the calculated coating thermal noise reduction factor (w.r.t. the current aLIGO design), for different values of the H' extinction coefficient, under the constraints $\tau_C \leq$ 6ppm and $\alpha_C \leq$ 1ppm.. Each design is identified by the couple of integers (N_t, N_b) representing the number of QWL doublets in the top and bottom stack.
The noise reduction achievable by the triplet-based optimal design discussed in the next Section is also shown for comparison. Note that noise reduction is quite effective even for relatively large values of the the extinction coefficient $\kappa_{H'}$.
Prototypes of optimized $SiO_2/Ti\!:\!Ta_2O_5/SiNx$ QWL coatings have been deposited and characterized

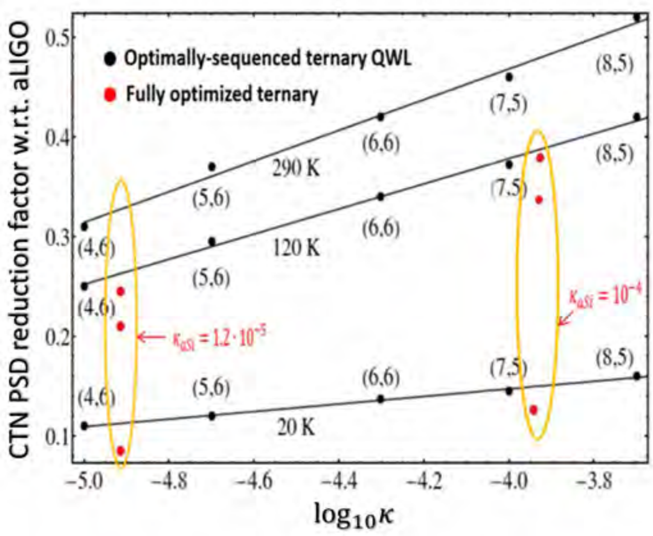

Рис. 2. Coating thermal noise PSD reduction factor (w.r.t. the current aLIGO design) for Silica/Ti-doped Tantala/aSilicon based ternary coatings with QWL layers, vs log of extinction coefficient of aSi. Three different operating temperatures (290, 120, and 20 K) are considered. The red markers refer to the optimized triplet-based design discussed in Section 3.2.

at LMA-CNRS, and their thermal noise has been measured using the MIT-CTN facility, with promising results [105].

3.1. Multiobjective M-ary Coating Optimization

Optimizing the design of M-ary coatings with $M > 2$ without any prior assumption on the coating structure requires a more general approach.
A coating design is fully specified by the set

$$\mathcal{D} = \{(m_k, \delta_k) | k = 1, 2, \ldots, N_T\} \tag{3.3}$$

where $m_k \in \mathbf{N}$ identifies the material making the $k-$th layer, out of a finite list of candidates, and $\delta_k \in (0, 1/2)$ is the optical thickness of the $k-$th layer. As already stated, the sought optimal design should minimize coating thermal noise (i.e., the coating loss angle ϕ_C) subject to the constraints[4]

$$\tau_C \leq \tau_0, \ \alpha_C \leq \alpha_0 \tag{3.4}$$

with typical (LIGO) values $\tau_C = 6$ppm and $\tau_C = 1$ppm.

This a constrained/multi-objective optimization problem with *conflicting* requirements. Such problems are most conveniently managed by constructing their Pareto (or tradeoff) manifold P [106]. In our case, P is a 2D-surface in the 3D-space $(\tau_C, \alpha_C, \phi_C)$ (objective-space). Each point of P corresponds to a coating design (a point in the design space) for which (3.4) are met; different points represent different tradeoffs among the conflicting requirements. The manifold P is the set of all *non-dominated designs*, i.e., those designs that are *better* than any other in terms of *at least one* objective, and *not worse* in terms of *all* other objectives.

Constructing the Pareto manifold is nontrivial: exhaustive sampling of the design space is unaffordable due to the combinatorial blow-up of the computational burden with the number of layers, and candidate materials. To attack the problem, meta-heuristics are used [107]- a branch of experimental (i.e., computer aided) Mathematics, that uses an arsenal of robust algorithmic tools like, e.g., evolutionary [108] and co-operative-agent [109] engines, to sample the manifold P as densely/uniformly as possible/needed, capitalizing on the accumulating knowledge about its structure.

To obtain the ternary optimized designs illustrated in the next Subsection we used a state-of-the-art meta-heuristics based tool [110], freely available to non-commercial users [111], that allows to set the desired resolution along each direction in the $(\tau_C, \alpha_C, \phi_C)$ space.

A typical Pareto manifold is shown in Figure 3, for the special case of a ternary coating using SiO_2, $Ti:Ta_2O_5$ and aSi with cSi substrate working at $\lambda = 1550nm$ and $T = 20K$. The manifold sections with $\tau_C = 6$ppm and $\alpha_C = 1$ppm are also shown, illustrating the corresponding tradeoff curves.

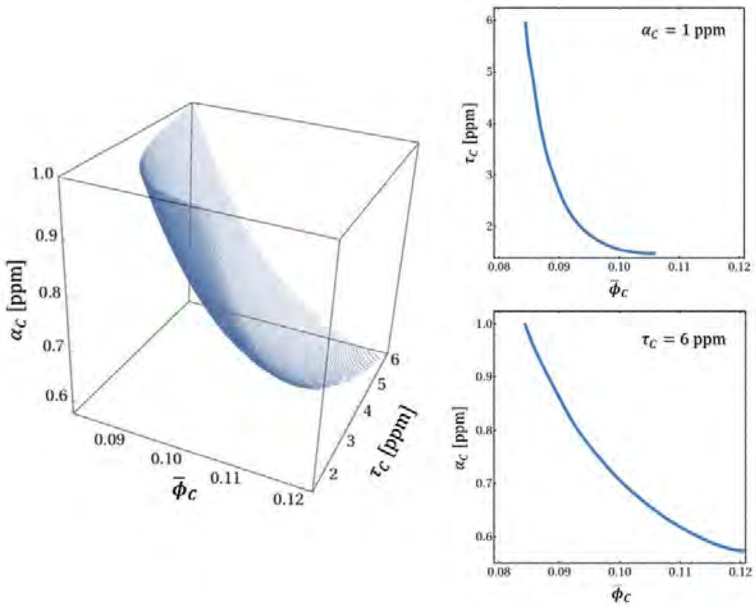

Рис. 3. Ternary coating using SiO_2, $Ti:Ta_2O_5$ and aSi with cSi substrate working at $\lambda = 1550nm$ and $T = 20K$. Left: computed Pareto manifold in the objective space ($\bar{\phi}_C$ is the coating loss angle scaled to the current aLIGO one). Right: its sections $\tau_C = 6$ppm and $\alpha_C = 1$ppm.

[4]Further constraints, e.g., requiring moderate reflectance at a second wavelength (for alignment purposes) and/or a reflection coefficients phase close to π at the working wavelength (so as to minimize the electric field on the coating face, and reduce contamination) may be also enforced.

3.2. Some New Results and Discussion

A systematic study of optimized ternary coatings using SiO_2 as the low-index (L) material, aSi or $SiNx$ for the large-extinction high-index material (H'), and different $(Ti{:}Ta_2O_5,\ Ti:SiO_2,\ Ti:GeO_2)$ for the high-index low extinction material (H) is ongoing, in the above described framework, based on the above framework and tools. A preliminary account can be found in [112].
The typical structure of an optimized ternary coating is illustrated in Figure 4. It consists of triplets $[L|H|H']$ satisfying Larruquert criterion. Close to the coating top and the substrate, the triplets degenerate into $[L|H]$ and $[L|H']$doublets, respectively. In between, there is a group of *bridging* triplets where as we move toward the substrate, the H layers get thinner, while the H' ones become thicker.

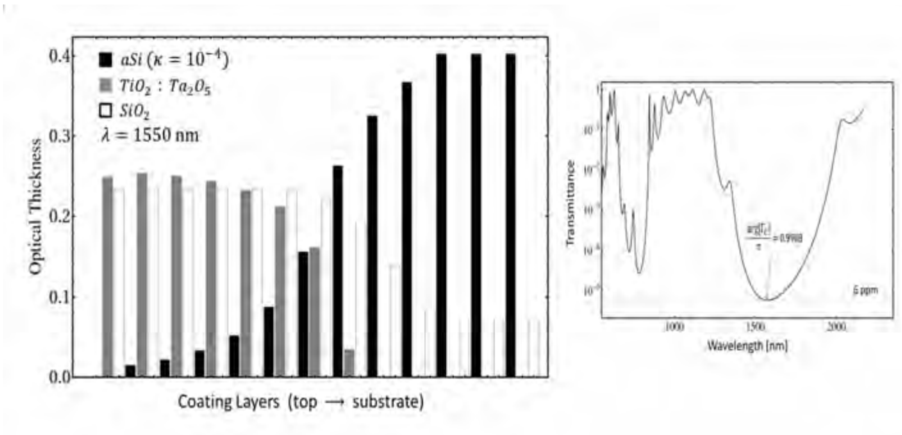

Рис. 4. Left: Typical structure of optimized ternary coating. The simulation assumes a cSi substrate and $T = 20K$. The calculated coating thermal noise PSD reduction factor w.r.t. the current aLIGO design is ≈ 0.126. Right: transmittance vs wavelength. Additional requirements on a second reflectance window, and on the phase of Γ_C at the working wavelength are satisfied.

The calculated CTN PSD reduction factor of a number of ternary coatings (both doublet and triplet based) using SiO_2, $Ti:SiO_2$ and aSi are collected in the following Table. As anticipated, the CTN

Таблица 1. Table I - CTN PSD reduction factor of some optimized ternary coatings fulfilling (3.4) w.r.t. the current aLIGO design.

L, H, H'	Substrate	λ [nm]	T[K]	$\kappa_{H'}$	CTN PSD reduction factor		
					Doublet based		Triplet based
					QWL	Bragg	
SiO_2, Ti:Ta_2O_5	SiO_2	1064	290	-	1	-	-
SiO_2, Ti:SiO_2	SiO_2	1064	290	-	0.67	-	-
SiO_2, Ti:SiO_2, *a*Si	SiO_2	1550	290	$1.\cdot 10^{-4}$	0.284	0.251	0.234
SiO_2, Ti:SiO_2, *a*Si	SiO_2	1550	290	$1.\cdot 10^{-3}$	0.373	0.337	0.324
SiO_2, Ti:SiO_2, *a*Si	cSi	1550	120	$1.\cdot 10^{-4}$	0.126	0.119	0.097
SiO_2, Ti:SiO_2, *a*Si	cSi	1550	120	$1.\cdot 10^{-3}$	0.163	0.151	0.141
SiO_2, Ti:SiO_2, *a*Si	cSi	1550	20	$1.\cdot 10^{-4}$	0.084	0.070	0.044
SiO_2, Ti:SiO_2, *a*Si	cSi	1550	20	$1.\cdot 10^{-3}$	0.108	0.088	0.068

reduction is quite good (and reaches the aLIGO+ goals) even for relatively large values of the aSi optical extinction.
As a conclusion, we stress that optimized multimaterial coatings may achieve superior performances in terms of CTN, under the given transmittance and absorbance requirements, compared to binary

coatings, using new materials at their present stage of development.

4. Conclusion and Recommendations

The science of HR coatings with extremely faible thermal noise has been developing in the last few years, driven by the GW detectors' Community. Its application potential is however not limited to GW detectors, but impacts several fields, including optical frequency standards, ultra-stable clocks, and estreme Metrology at large.

Substantial efforts have been made during the last two decades, and important results have been achieved. Many research directions and tools remain to be explored, though. Studying the properties of more glass-forming materials, e.g., TeO_2, and using powerful material modeling tools like, e.g., Kramers-Konig and universal-relaxation relationships may offer new insight into the physics of low-noise optical coatings, and open new directions.

Acknowledgments

I'm indebted with many Colleagues for fruitful cooperation, and in particular with S. Chao (NTHU), R. DeSalvo, V. Pierro and M. Principe (Sannio U), who co-authored with me most of the papers on coating optimization and nanolayered materials. The results in Sect. 3 are largely based on V. Pierro's extensive coding and simulation work. Valuable discussions with M. Granata, Ch. Michel, L. Mereni, L. Pinard and B. Sassolas all from LMA, from N. Demos (MIT), A. Gretarsson (ERAU), G. Harry (AU), I. Martin, G. McGhee and S. Tait (U Glasgow), E.D. Black and G. Vajente (Caltech), J. Steinlechner (Maastricht U), L. Bellon (ENS Lyon), G. Cagnoli (UCB Lyon), and all fellow members of the USannio/UniSA LVK groups are acknowledged.

Special thanks are due to the PIRT-23 Organizers for their kind invitation, and the highly professional BMSTU Staff for continued support. Большое спасибо !

This work has been funded in part by Italy's National Institute for Nuclear Physics (INFN).

Список литературы/References

1. J. Aasi et al., Advanced LIGO, *Class. Quantum Grav.* 32 (2015) 074001
2. F. Acernese et al., Advanced Virgo: a 2nd Generation GW Detector, *Class. Quantum Grav.* 32 (2015) 024001
3. T. Akutsu et al., Overview of KAGRA: Detector Design and Construction History, *Progr. Th. Experim. Phys.* 2021 (2021) 05A101
4. LSC, Instrument Science White Paper, *LIGO Document T2200384* (2022) `https://dcc.ligo.org/LIGO-T2200384`
5. S. Gossler et al., Coating-Free Mirrors for High Precision Interferometric Experiments, *Phys. Rev.* A76 (2007) 053810
6. A.G. Gurkovsky et al., Reducing Thermal Noise in Future Gravitational Wave Detectors by Employing Khalili Etalons, *Phys. Lett. A.* 375 (2011) 4147
7. D. Heinert et al., Calculation of Thermal Noise in Grating Reflectors, *Phys. Rev. D.* 88 (2013) 042001
8. I.M. Pinto, M. Principe, R. DeSalvo, Reflectivity and Thickness Optimization, Ch. 12 in *Optical Coatings and Thermal Noise in Precision Measurements,* G. Harry et al., Eds., Cambridge Univ. Press, Cambridge (UK), 2012, ISBN 978-1-107-00338-5.
9. D.R.M. Crookes et al., Experimental Measurements of Mechanical Dissipation Associated with Dielectric Coatings Formed Using SiO_2 , Ta_2O_5 and Al_2O_3, *Class. Quantum Grav.* 23 (2006) 4953
10. G M. Harry, Material Downselect Rationale and Directions, *LIGO Document G-G050088-00-R* `https://dcc.ligo.org/DocDB/0035/G050088/000/G050088-00.pdf`

11. A.F. Brooks et al., Direct Measurement of Absorption-Induced Wavefront Distortion in High Optical Power Systems, *Appl. Opt.* 48 (2009) 355
12. G.M. Harry et al., Titania-Doped Tantala/Silica Coatings for Gravitational-Wave Detection, *Class. Quantum Grav.* 24 (2007) 405
13. R. Flaminio et al., A Study of Coating Mechanical and Optical Losses in View of Reducing Mirror Thermal Noise in Gravitational Wave Detectors, *Class Quantum Grav.* 27 (2010) 084030
14. R.M. Netterfeld, M. Gross, Investigation of Ion-Beam-Sputtered Silica-Titania Mixtures for Use in Gravitational Wave Interferometer Optics, *Proc. OSA-OIC-2007*, paper ThD2
15. J. Franc et al., Mirror Thermal Noise in Laser Interferometer Gravitational Wave Detectors Operating at Room and Cryogenic Temperature, Einstein Telescope Note ET-021-09, *arXiv:0912.0107*
16. M. Granata et al., Optical and Mechanical Properties of Ion-Beam-Sputtered MgF_2 Thin Films for Gravitational-Wave Interferometers, *Phys. Rev. Appl.* 17 (2022) 034058
17. M. Bischi et al., Characterization of Ion-Beam-Sputtered AlF_3 Thin Films for Gravitational-Wave Interferometers, *Phys. Rev. Applied* 18 (2022) 054074
18. G. Favaro et al., Measurement and Simulation of Mechanical and Optical Properties of Sputtered Amorphous SiC Coatings, *Phys. Rev. Appl.* 18 (2022) 044030
19. M. Segreti et al., Mechanical and Optical Characterization of Sputtered Amorphous GaN Thin Film for High-Reflectvity and Low-Loss Coatings, GWADW 2023 (poster) , `https://agenda.infn.it/event/32907/contributions/200157/attachments/106040/149266/Poster_versione6-2.pdf`
20. K. Craig et al., Mirror Coating Solution for the Cryogenic Einstein Telescope, *Phys. Rev. Lett.* 122 (2019) 231102 1
21. M. Fazio et al., Growth and Characterization of Sc_2O_3 Doped Ta_2O_5 Thin Films, *Appl. Opt.* 5 (2020) A106
22. A. Amato et al., Optical and Mechanical Properties of Ion-Beam-Sputtered Nb_2O_5 and $TiO_2 - Nb_2O_5$ Thin Films for Gravitational-Wave Interferometers and an Improved Measurement of Coating Thermal Noise in Advanced LIGO, *Phys. Rev. D.* 103 (2021) 072001
23. M. Abernathy et al., Exploration of Co-sputtered $Ta_2O_5 - ZrO_2$ Thin Films for Gravitational Wave Detectors, *Class. Quantum Grav.* 38 (2021) 195021
24. E. Lalande et al., Zirconia-Titania-Doped Tantala Optical Coatings for Low Mechanical Loss Bragg Mirrors, *J. Vac. Sci. Technol. A.* 39 (2021) 1
25. M. Granata et al., Progress in the Measurement and Reduction of Thermal Noise in Optical Coatings for Gravitational-Wave Detectors , *Appl. Opt.* 59 (2020) A229
26. M. Fazio et al., Comprehensive Study of Amorphous Metal Oxide and Ta_2O_5-based Mixed Oxide Coatings for Gravitational-Wave Detectors, *Phys. Rev. D* 105 (2022) 102008,
27. G. Vajente et al., Low Mechanical Loss TiO2:GeO2 Coatings for Reduced Thermal Noise in Gravitational Wave Interferometers, *Phys. Rev. Lett.* 127 (2021) 071101
28. S. Khadka et al.,Cryogenic Mechanical Loss of Amorphous Germania and Titania-Doped Germania Thin Films, *Class. Quantum Grav.* 40 (2023) 205002
29. A. Davenport, Investigation of $TiO_2 : GeO_2$ for High Reflector Stacks, *LIGO document G2302140*, `https://dcc.ligo.org/LIGO-G2302140`
30. E. Lalande et al, Ar Transport and Blister Growth Kinetics in Titania-doped Germania-based Optical Coatings, *LIGO Document P2300328*, `https://dcc.ligo.org/LIGO-P2300328`
31. G.I. McGhee et al., Titania Mixed with Silica: A Low Thermal-Noise Coating Material for Gravitational-Wave Detectors, *Phys. Rev. Lett.* 131 (2023) 171401

32. I.M. Pinto et al., nm-Layered Amorphous Glassy Oxide Composites for 3rd Generation Interferometric Gravitational Wave Detectors, *LIGO Document-G1401358* (2014), `https://dcc.ligo.org/DocDB/0116/G1401358/001/G1401358.pdf`

33. H.-W. Pan et al., Thickness-Dependent Crystallization on Thermal Anneal for Titania/Silica nm-Layer Composites Deposited by Ion-Beam Sputter Method, *Opt. Express* 22 (2014) 29847

34. P. Amico et al., Investigation on Mechanical Losses in TiO_2/SiO_2 Dielectric Coatings, *J. Phys. Conf. Ser.* 32 (2006) 413

35. L.-C. Kuo et al., Low Cryogenic Mechanical Loss Composite Silica Thin Film for Low Thermal Noise Dielectric Mirror Coatings, *Optics Lett.* 44 (2019) 247

36. L.-C. Kuo et al., Annealing Effect on the Nano-meter Scale Titania/Silica Multi-layers for Mirror Coatings of the Laser Interferometer Gravitational Waves Detector, *Proc. of the 2019 PhotonIcs & Electromagnetics Research Symposium (PIERS),* p. 2347

37. I. Pinto, Which Nanolayers are Worth a Try,, LIG*O Document G2000413* (2020) `https://dcc.ligo.org/LIGO-G2000413`

38. I. Pinto, Nanolayered Silica/Alumina Composites, *LIGO Document G2001499* (2020) `https://dcc.ligo.org/LIGO-G2001499`

39. B. Larsen et al., Crystallization in Zirconia Film Nano-Layered with Silica, *Nanomaterials* 11 (2021) 344

40. Le Yang et al., Structural Evolution that Affects the Room-Temperature Internal Friction of Binary Oxide Nanolaminates: Implications for Ultrastable Optical Cavities, ACS Appl. *Nano Mater.* 3 (2020) 12308

41. M. Steinecke et al., Quantizing Nanolaminates as Versatile Materials for Optical Interference Coatings, *Appl. Optics* 59 (2020) A236

42. D.E. Aspnes, Local Field Effects and Effectve-Medium Theory: a Microscopic Perspective, *Am. J. Phys.* 50 (1981) 704

43. O. Stenzel et al., Mixed Oxide Coatings for Optics, *Appl. Opt.* 50 (2011) C69

44. S. Barta, Effective Young's Modulus and Poisson's Ratio for the Particulate Composite, *J. Appl. Phys.* 75 (1994) 3258

45. M. Principe et al., Material Loss Angles from Direct Measurements of Broadband Thermal Noise, *Phys. Rev. D.* 91 (2015) 022005

46. K.S. Gilroy, W.A. Phillips, An Asymmetric Double-Well Potential Model for Structural Relaxation Processes in Amorphous Materials, *Phil. Mag. B.* 43 (1981) 735

47. A. Amato et al., Observation of a Correlation Between Internal Friction and Urbach Energy in Amorphous Oxides Thin Films, *Sci. Rep.* 10 (2020) 1670

48. R. Bassiri et al., Correlations Between the Mechanical Loss and Atomic Structure of Amorphous TiO_2-doped Ta_2O_5 Coatings, *Acta Mater.* 61 (2013) 1070

49. J.P. Trinastic et al., Molecular Dynamics Modeling of Mechanical Loss in Amorphous Tantala and Titania-Doped Tantala, *Phys. Rev. B.* 93 (2016) 014105

50. T. Damart, D. Rodney, Atomistic Study of Two-level Systems in Amorphous Silica, *Phys. Rev. B.* 97 (2018) 014201

51. K. Prasai et al., Annealing-Induced Changes in the Atomic Structure of Amorphous Silica, Germania, and Tantala Using Accelerated Molecular Dynamic, *Phys. Stat. Sol. B.* 258 (2021) 2000519

52. J. Jiang et al., Amorphous Zirconia-doped Tantala Modeling and Simulations using Explicit Multi-Element Spectral Neighbor Analysis Machine Learning Potentials (EME-SNAP), *Phys. Rev. Mater.* 7 (2023) 045602

53. M. Kim et al., Atomic Structure Characterization of Titania-doped Germania, *LIGO Document G2301799*, `https://dcc.ligo.org/LIGO-G2301799`
54. M. Turowski, et al., Practice-Oriented Optical Thin Film Growth Simulation via Multiple Scale Approach, *Thin Solid Films* 592 (2015) 240
55. F.V. Grigoriev, V.B. Sulimov, A.V.Tikhonravov, Application of a Large-Scale molecular dynamics approach to modelling the Deposition of TiO_2 Thin Films, *Computat. Mater. Sci.* 188 (2021) 110202
56. F.V. Grigoriev, V.B. Sulimov,Atomistic Simulation of Physical Vapor Deposition of Optical Thin Films, *Nanomaterials*, 13 (2023) 1717
57. A. Alexandrovski et al., Photothermal Common-Path Interferometry (PCI): New Developments, *SPIE Proceedings* 7193 (2009) 71930D
58. K.V. Vlasova et al., High-sensitive Absorption Measurement in Transparent Isotropic Dielectrics with Time-resolved Photothermal Common-Path Interferometry, *Appl. Opt.*, 57 (2018) 6318
59. J.R. Smith et al., Apparatus to Measure Optical Scatter of Coatings Versus Annealing Temperature, *Proc. OSA-OIC* 2019, FA.2
60. G.H. Ogin et al., Measuring the Thermo-Optic Response of Dielectric Stack Mirrors, *Proc. OSA-OIC* 2016, MB.7
61. E.M. Gretarsson, A.M. Gretarsson, Three Methods for Characterizing Thermo-Optic Noise in Optical Cavities, *Phys. Rev. D.* 98 (2018) 122004
62. E. Cesarini et al., A ‘Gentle’ Nodal Suspension for Measurements of the Acoustic Attenuation in Materials, *Rev. Sci. Instrum.* 80 (2009) 053904
63. G. Vajente et al., Method for the Experimental Measurement of Bulk and Shear Loss Angles in Amorphous Thin Films, *Phys. Rev. D.* 101 (2020) 042004
64. K. Numata et al., Wide-Band Direct Measurement of Thermal Fluctuations in an Interferometer, *Phys. Rev. Lett.* 91 (2003) 260602
65. E.D. Black et al., Direct Observation of Broadband Coating Thermal Noise in a Suspended Interferometer, *Phys. Lett. A.* 328 (2004) 1
66. T. Chalermsongsak et al., Broadband Measurement of Coating Thermal Noise in Rigid Fabry–Perot Cavities, *Metrologia* 52 (2015) 17
67. S. Gras, M. Evans, Direct Measurement of Coating Thermal Noise in Optical Resonators, *Phys. Rev. D* 98 (2018) 122001
68. R. Pedurand, Instrumentation for Thermal Noise Spectroscopy, PhD Thesis (2019), Univ. Lyon (FR), 2019, `https://theses.hal.science/tel-02612035`
69. G.D. Cole et al., Tenfold Reduction of Brownian Noise in High-Reflectivity Optical Coatings, *Nature Photonics* 7 (2013) 644
70. A.C. Lin et al., Epitaxial Growth of GaP/AlGaP Mirrors on Si for Low Thermal Noise Optical Coatings, Opt. *Mater. Express* 8 (2015) 1890
71. A.V. Cumming et al., Measurement of the Mechanical Loss of Prototype GaP/AlGaP Crystalline Coatings for Future Gravitational Wave Detectors, *Class. Quantum Grav.* 32 (2015) 035002
72. P.G. Murray et al., Cryogenic Mechanical Loss of a Single-Crystalline GaP Coating Layer for Precision Measurement Applications, *Phys. Rev. D.* 95 (2017) 042004
73. G.D. Cole et al., High-Performance Near- and Mid-Infrared Crystalline Coatings, *Optica* 3 (2016) 647
74. G.D. Cole et al., Substrate-Transferred GaAs/AlGaAs Crystalline Coatings for Gravitational-Wave Detectors, *Appl. Phys. Lett.* 122 (2023) 110502
75. M.L. Gorodetsky, Thermal Noises and Noise Compensation in High-Reflection Multilayer Coating, *Phys. Lett. A.* 372 (2008) 6813

76. M. Evans et al., Thermo-Optic Noise in Coated Mirrors for High-Precision optical Measurements, *Phys. Rev. D.* 78 (2008) 102003
77. T. Chalermsongsak et al., Coherent Cancellation of Photothermal Noise in $GaAs/Al_{0.92}Ga_{0.08}As$ Bragg Mirrors, *Metrologia* 53 2016 860
78. S. Kryhin, E.D. Hall, V. Sudhir, Thermorefringent Noise in Crystalline Optical Materials, *Phys. Rev. D.* 107 (2023) 022001
79. J. Yu et al., Excess Noise and Photoinduced Effects in Highly Reflective Crystalline Mirror Coatings, *Phys. Rev. X.* 13 (2023) 041002
80. H.-W. Pan et al., Silicon Nitride Films Fabricated by a Plasma-Enhanced Chemical Vapor Deposition Method for Coatings of the Laser Interferometer Gravitational Wave Detector, *Phys. Rev. D.* 87 (2018) 022004
81. D.-S. Tsai et al., Amorphous Silicon Nitride Deposited by an NH_3-free Plasma Enhanced Chemical Vapor Deposition Method for the Coatings of the Next Generation Laser Interferometer Gravitational Waves Detector, *Class. Quantum Grav.* 39 (2022) 15LT01
82. G.S. Wallace et al., Non-stoichiometric Silicon Nitride for Future Gravitational Wave Detectors, *LIGO Document P-2300539* (2023), https://dcc.ligo.org/LIGO-P2300359
83. P. G. Murray et al., Ion-beam Sputtered Amorphous Silicon Films for Cryogenic Precision Measurement Systems, *Phys. Rev. D* 92 (2015) 062001
84. J. Steinlechner et al., Optical Absorption of Ion-Beam Sputtered Amorphous Silicon Coatings, *Phys. Rev. D* 93 (2016) 062005
85. J. Steinlechner et al., Silicon-Based Optical Mirror Coatings for Ultrahigh Precision Metrology and Sensing, *Phys. Rev. Lett.* 120 (2018) 3602
86. R. Birney et al., Amorphous Silicon with Extremely Low Absorption: Beating Thermal Noise in Gravitational Astronomy, *Phys. Rev. Lett.* 121 (2018) 191101
87. L. Terkowsky et al., Influence of Deposition Parameters on the Optical Absorption of Amorphous Silicon Thin Films, *Phys. Rev. Res.* 2 (2020) 033308
88. M. Molina-Ruiz, Hydrogen-Induced Ultralow Optical Absorption and Mechanical Loss in Amorphous Silicon for Gravitational-Wave Detectors, *Phys. Rev. Lett.* 131 (2023) 256902
89. M. Kinley-Hanlon et al., Update on Nanolayer aSi/SiO_2 Coatings and Ion Implantation (SIMOX) Layers for Mechanical Loss,*LIGO Document G2300684* (2023) https://dcc.ligo.org/LIGO-G2300684
90. A. V. Vinogradov and Ya. B. Zel'dovich, X-ray and Far UV Multilayer Mirrors: Principles and Possibilities, *Appl. Opt.*, 16 (1977) pp. 89-93
91. J.I. Larruquert, Reflectance Enhancement in the Extreme Ultraviolet and Soft X Rays by Means of Multilayers with More than Two Materials, *J. Opt. Soc. Am.* 19 (2002) pp. 391-397
92. J.I. Larruquert. Inreflectance: a New Function for the Optimization of Multilayers with Absorbing Materials, *J. Opt. Soc. Am.* A22 (2005) 1607.
93. J.I. Larruquert et al., Constructing Multilayers with Absorbing Materials, *Chinese Opt. Lett.* 8 (2010) 159
94. J. Agresti et al., Optimized Multilayer Dielectric Mirror Coatings for Gravitational Wave Interferometers, *Proc. of SPIE*, 6286 (2006) 628608,
95. A.E. Villar et al., Measurement of Thermal Noise in Multilayer Coatings with Optimized Layer Thickness, *Phys. Rev. D* 81 (2010) 122001
96. L.Pinard et al., Mirrors Used in the LIGO Interferometers for First Detection of Gravitational Waves, *Appl. Optics* 56 (2017) C11
97. D.V. Martynov et al., Sensitivity of the Advanced LIGO Detectors at the Beginning of Gravitational

Wave Astronomy, *Phys. Rev. D.* 93 (2016) 112004,

98. N.M. Kondratiev, A.G. Gurkovsky, M.L. Gorodetsky, Thermal Noise and Coating Optimization in Multilayer Dielectric Mirrors, *Phys. Rev. D.* 84 (2011), 022001
99. V. Pierro et al., On the Performance Limits of Coatings for Gravitational Wave Detectors Made of Alternating Layers of Two Materials, *Optical Mater.* 96 (2019) 109269
100. J. Steinlechner et al., Thermal Noise Reduction and Absorption Optimization via Multimaterial Coatings, *Phys. Rev. D* 91 (2015) 042001
101. W. Yam, S. Gras, M. Evans, Multimaterial Coatings with Reduced Thermal Noise, *Phys. Rev. D* 91 (2015) 042002
102. J. Steinlechner, I.W. Martin, High Index Top Layer for Multimaterial Coatings, *Phys. Rev. D.* 93 (2016) 102001
103. S. Tait et al., 'Demonstration of the Multimaterial Coating Concept to Reduce Thermal Noise in Gravitational-Wave Detectors, *Phys. Rev. Lett.* 125 (2020) 011102
104. V. Pierro et al., Ternary Quarter Wavelength Coatings for Gravitational Wave Detector Mirrors: Design Optimization via Exhaustive Search, *Phys. Rev. Res.* 3 (2021) 023172
105. M. Granata et al., Present Results and Future Perspectives of SiNx-based Multi-Material Mirror Coatings, *LIGO Document G2300642* `https://dcc.ligo.org/LIGO-G2300642`
106. C.A. Coello-Coello et al., Evolutionary Multiobjective Optimization: Open Research Areas and Some Challenges Lying Ahead , *Complex & Intelligent Sys.* 6 (2020) 221
107. C. Blum, A. Roli, Metaheuristics in Combinatorial Optimization: Overview and Conceptual Comparison, ACM *Comput. Surv.* 35 (2003) 268
108. A. Konak, D.W. Coit, A.E. Smith, Multi-Objective Optimization Using Genetic Algorithms: A Tutorial, *J. RESS* 91 (2006) 992
109. M. Dorigo et al., Ant Colony Optimization: Artificial Ants as a Computational Intelligence Technique, *IEEE Computat. Intell. Mag.*, 1 (2006) 28
110. D. Hadka , P.M. Reed , BORG: An Auto-Adaptive Many-Objective Evolutionary Computing Framework, *Evolutionary Computation* 21 (2013) 231
111. `http://borgmoea.org/`
112. I.M. Pinto et al., Optimized Ternary Coatings : Options and Performance, *LIGO Document G2201509* `https://dcc.ligo.org/LIGO-G2201509`
113. R. Schnabel et al., Building Blocks for Future Detectors: Silicon Test Masses and 1550 nm Laser Light, *J. Phys. Conf. Ser.* 228 (1010) 012029.
114. R.X. Adikhari et al.,A Cryogenic Silicon Interferometer for Gravitational-wave Detection, *Class. Quantum Grav.* 37 (2020) 165003
115. P.R. Saulson, *Fundamentals of Interferometric Gravitational Wave Detectors,* World Scientific, Singapore, 2017, ISBN 978-9813143074
116. Yu. Levin, Internal Thermal Noise in the LIGO Test Masses: a Direct Approach, *Phys. Rev D.* 57 (1998) 659
117. M.L. Gorodetsky, Thermal Noises and Noise Compensation in High-Reflection Multilayer Coating, *Phys. Lett. A.* 372 (2008) 6813
118. V.B. Braginsky, M.L. Gorodetsky, S.P. Vyatchanin, Compendium of Thermal Noises in Optical Mirrors, Ch. 3 in *Optical Coatings and Thermal Noise in Precision Measurements,* G. Harry et al. (Eds.), Cambridge Univ. Press, Cambridge (UK), 2012, ISBN 978-1-107-00338-5.
119. G.M. Harry et al., Optical Coatings for Gravitational Wave Detection, *Proc. SPIE* 5527 (2004) 33
120. A.G. Gurkovsky and S.P. Vyatchanin, The Thermal Noise in Multilayer Coatings, *Phys. Lett. A.* 374 (2010) 3267

121. M. Fejer, Effective Medium Description of Multilayer Coatings , *LIGO Document T-T2100186*, https://dcc.ligo.org/LIGO-T2100186

122. K. Somiya, K. Yamamoto, Coating thermal Noise of a Finite-Size Cylindrical Mirror, *Phys. Rev. D.* 79 (2009) 102004

123. T. Hong et al., Brownian Thermal Noise in Multilayer Coated Mirrors, *Phys. Rev. D.* 87 (2013) 082001

124. V. Pierro et al., Perspectives on Beam-Shaping Optimization for Thermal-Noise Reduction in Advanced Gravitational-Wave Interferometric Detectors: Bounds, Profiles, and Critical Parameters, *Phys. Rev. D.* 76 (2007) 122003

125. https://cosmicexplorer.org/

126. https://apps.et-gw.eu/tds/?call_file=ET-0028A-20_EinsteinTelescopeScienceCaseDe.pdf

127. I.W. Martin et al., Low Temperature Mechanical Dissipation of an Ion-Beam Sputtered Silica Film, *Class. Quantum Grav.* 31 (2014) 035019

128. I.W. Martin et al., Comparison of the Temperature Dependence of the Mechanical Dissipation in Thin Films of Ta_2O_5 and Ta_2O_5 doped with TiO_2, *Class. Quantum Grav.* 26 (2009) 155012

129. M. Granata et al., Cryogenic Measurements of Mechanical Loss of High-Reflectivity Coating and Estimation of Thermal Noise, *Optics Lett.* 38 (2013) 5268

130. E. Hirose et al., Mechanical Loss of a Multilayer Tantala/Silica Coating on a Sapphire Disk at Cryogenic Temperatures: Toward the KAGRA Gravitational Wave Detector, *Phys. Rev. D.* 90 (2014) 102004

Appendix A - Coating Reflection and Absorption

Let the coating operate in vacuum, and consist of N_T homogeneous plane layers laid on a homogeneous half-space, as sketched in Figure A1.

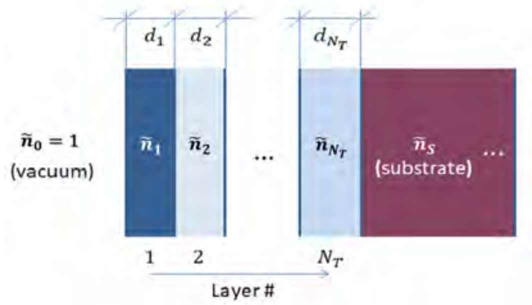

Рис. A1. Coating structure and notation

For a monochromatic, locally plane-wave with normal incidence, the transmission matrix of the m-th layer is [8]

$$\mathbf{T}_m = \begin{bmatrix} \cos(\psi_m) & (\imath/\tilde{n}_m)\sin(\psi_m) \\ \imath\tilde{n}_m \sin(\psi_m) & \cos(\psi_m) \end{bmatrix}, \tag{A.1}$$

where

$$\psi_m = \frac{2\pi}{\lambda_0}\tilde{n}_m d_m, \tag{A.2}$$

is the layer (complex) phase-thickness, d_m being its metric thickness,

$$\tilde{n}_m = n_m - \imath\kappa_m, \tag{A.3}$$

its complex refractive index, and λ_0 the free-space wavelength [5]. An $\exp(\imath\omega_0 t)$ time dependence is understood. The transmission matrix (A.1) connects the electromagnetic fields at the input (left, in Figure A1) and output (right) face of the m-layer as follows:

$$\begin{bmatrix} E^{(m)} \\ Z_0 E^{(m)} \end{bmatrix} = \mathbf{T}_m \begin{bmatrix} E^{(m+1)} \\ Z_0 H^{(m+1)} \end{bmatrix}, \tag{A.4}$$

Z_0 being the free-space characteristic impedance.
The coating optical response is fully described by its transmission matrix $\mathbf{T}$,

$$\mathbf{T} = \mathbf{T}_1 \cdot \mathbf{T}_2 \cdot \dots \cdot \mathbf{T}_{N_T}. \tag{A.5}$$

The equivalent (complex) refractive index of the whole substrate-terminated coating is,

$$\tilde{n}_C = \frac{T_{21} + \tilde{n}_S T_{22}}{T_{11} + \tilde{n}_S T_{12}}, \tag{A.6}$$

whence the coating reflection coefficient and power transmittance can be written:

$$\Gamma_C = \frac{1-\tilde{n}_C}{1+\tilde{n}_C}, \ \tau_C = \frac{\mathcal{P}_{\text{in}}}{\mathcal{P}^+} = 1 - |\Gamma_c|^2, \tag{A.7}$$

$\mathcal{P}_{\text{in}}$ being the power density (power per unit area) flowing into the coating face, and $\mathcal{P}^+$ the power density of the incident wave,

$$\mathcal{P}^+ = \frac{1}{2Z_0}|E_{\text{inc}}|^2. \tag{A.8}$$

The power density dissipated in the coating is

$$\mathcal{P}_{in} - \mathcal{P}_{out}, \tag{A.9}$$

where

$$\mathcal{P}_{\text{out}} = \frac{1}{2}\text{Re}[E^{(S)}H^{(S)*}] \tag{A.10}$$

is the power density flowing into the substrate, $E^{(S)}$ and $H^{(S)}$ being the electric and magnetic fields at the coating/substrate interface,

$$\begin{bmatrix} E^{(S)} \\ Z_0 H^{(S)} \end{bmatrix} = \mathbf{T}^{-1} \begin{bmatrix} E^{(0)} \\ Z_0 H^{(0)} \end{bmatrix} = \mathbf{T}^{-1} \begin{bmatrix} E_{\text{inc}}(1+\Gamma_C) \\ E_{\text{inc}}(1-\Gamma_C) \end{bmatrix}. \tag{A.11}$$

The coating absorbance is therefore

$$\alpha_C = \frac{(\mathcal{P}_{\text{in}} - \mathcal{P}_{\text{out}})}{\mathcal{P}^+}. \tag{A.12}$$

Typical design values for the HR coatings of interferometric detectors of gravitational waves are $\tau_C \approx 5ppm$ and $\alpha_C \approx 1ppm$. Transmittance affects the light-storage time (and bandwidth) and the effective optical path-length (and minimum detectable GW geodetic deviation) of the detector; absorbance originates thermal-lensing mirror distortion, that should be actively compensated to avoid alignment loss [115].

Appendix B - Coating Thermal Noise

The power spectral density (PSD) of coating thermal noise can be derived from the fluctuation-dissipation theorem [116].
Coating thermal noise has multiple origins [117], [118]. We restrict here to Brownian noise, which turns out to be dominant for amorphous metal-oxides based coatings, and assume the same coating structure

[5] Running GW detectors use a 1064nm laser sources; future interferometers may use 1550nm [113] or 2000nm sources [114].

as in Figure A1.
The frequency dependent power spectral density $S^{(B)}_{\rm coat}(f)$ of coating thermal noise can be written :

$$S^{(B)}_{\rm coat}(f) = \frac{2k_BT}{\pi^2 w^2 f}\sum_{k=1}^{N_T} b_k d_k, \tag{B.1}$$

where k_B is Boltzmann constant, T the (absolute) temperature, w the (assumed Gaussian) laser-beam waist, f the frequency, d_k the metric thicknesses of the k-th coating layer, and

$$b_k = \frac{\phi_k}{Y_S}\left[\frac{Y_S}{Y_k}\frac{(1+\nu_k)(1-2\nu_k)}{1-\nu_k} + \frac{Y_k}{Y_S}\frac{(1+\nu_S^2)(1-2\nu_S^2)}{(1-\nu_k^2)}\right], \tag{B.2}$$

ϕ, Y and ν being the mechanical loss angle and the elastic Young and Poisson moduli, and the suffixes k and S referring to the k-th layer and the substrate, respectively.
Equation (B.1) is often rewritten in terms of a whole-coating loss angle ϕ_C as

$$S^{(B)}_{\rm coat}(f) = \frac{2k_BT}{\pi^{3/2} w f Y_S}\phi_C, \text{with } \phi_C = \frac{1}{\pi^{1/2}}\sum_{k=1}^{N_T}\phi_k\frac{d_k}{w}\left[\frac{Y_S}{Y_k}\frac{(1+\nu_k)(1-2\nu_k)}{1-\nu_k} + \frac{Y_k}{Y_S}\frac{(1+\nu_S^2)(1-2\nu_S^2)}{(1-\nu_k^2)}\right]. \tag{B.3}$$

Equation (B.2) was independently derived in [119] in terms of the elastic moduli for parallel and perpendicular stresses, and in [120], from first principles. More recently, it has been re-obtained in [121], using an effective-medium approach[6]. Equation (B.2) neglects correlation between intra-layer (1st term) and layer-substrate (2nd term) fluctuations, and other subtler effects discussed in [117] - [123].
It is seen from (B.1) that CTN could be reduced by increasing w, i.e., the illuminated area (see [124] for a broad discussion), and/or reducing temperature T - a choice made, e.g., for KAGRA and the planned Cosmic Explorer [125]and ET [126] detectors. It should be noted that mechanical loss-peaks at cryo temperatures are observed (with a few notable exceptions, including TiO_2) in most coating materials, including SiO_2 [127] and Ta_2O_5 [128] films [7].
The following remarks are in order:

- material noisyness should *not* be gauged on the basis of the mechanical loss angle ϕ_k alone (a frequent/persistent mistake in the technical Literature), since the b_k coefficients (B.2) are strongly dependent on the Young modulus ratio Y_k/Y_S as well (the Poisson moduli have a lesser impact, as seen from Figure B1, being $\nu \approx 0.25$ for all materials of interest);
- computation of the b_k via eq. (B.2) requires accurate knowledge of the elastic moduli and loss angles of the coating materials - which isn't available for many materials of potential interest (the situation is even worse for more complicated noise models, like, e.g., in [123], that depend on additional material parameters);
- loss angle measurements based on mechanical ringdown experiments on single- vs. multi-layer coatings lead to inconsistent results (see the discussion in Sect. V of [45]), for reasons yet to be understood;
- equation (B.1) can be seen as an *operational definition* of the material-dependent coefficients b_k. These latter can be cheaply retrieved from direct thermal noise PSD measurements made on a suitable number of different coatings that use the same layer materials, with different total thicknesses. In this connection, several instruments for the direct measurement of coating thermal noise PSD have been devised and built in recent years - see, e.g., [64] - [66], and some are currently in operation [67], [68].

[6] In ref [121] the coefficients B.2 are also written in terms of the bulk and shear elastic moduli.
[7] Cryogenic mechanical loss measurements on multilayer HR films laid on different substrates gave contradictory results [129], [130], for yet unclear reasons.

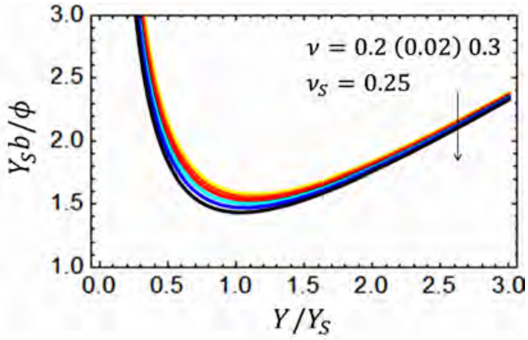

Рис. B1. Coating noise coefficient dependence on Y/Y_S for various ν values and $\nu_S = 0.25$.

Авторы

Пинто Иноченцо М., Итальянский национальный институт ядерной физики (INFN); ЛВК Научное сотрудничество; Университет имени Федерико II, Неаполь 80138, Италия (Профессор пенсионер).
E-mail: pinto@sa.infn.it

Просьба ссылаться на эту статью следующим образом:
Пинто И. М. Снижение теплового шума зеркал в детекторе гравитационных волн. Краткий обзор и некоторые новые результаты. *Пространство, время и фундаментальные взаимодействия.* 2023. № 3-4. С. 229–246.

Authors

Pinto Innocenzo M., Istituto Nazionale di Fisica Nucleare (INFN); LVK Scientific Collaboration; University Federico II, Naples 80138, Italy (retired professor).
E-mail: pinto@sa.infn.it

Please cite this article in English as:
Pinto I. M. Reducing Thermal Noise in the Mirrors of Gravitational Wave Detectors. A Short Review and Some New Results. *Space, Time and Fundamental Interactions*, 2023, no. 3-4, pp. 229–246.